



CPW Fed Dual Band Dual Sense Circularly Polarized Asymmetrical Y- Shaped Microstrip Patch Antenna for Wireless Applications

Mandar P. Joshi^{1*}, Vitthal J. Gond² and Jayant J. Chopade³

¹Dept. of E & TC, GES's R. H. Sapat College of Engineering, M. S. and R., Nashik, India

²Prof. & Head, Dept. of E & TC, MET's Institute of Engineering, Nashik, India,

³Dept. of E & TC, Matoshri College of Engineering & Research Centre, Nashik, India

*E-mail: mandarjoshi11@gmail.com

Abstract- This paper presents, coplanar waveguide (CPW) fed novel dual asymmetrical Y- shaped microstrip patch antenna with wide impedance bandwidth for wireless communication applications. The antenna offers wide impedance bandwidth of ($S_{11} < -10$ dB) 2.88 GHz with dual band dual sense circularly polarized response at 3.5 GHz and 4.9 GHz. The simulated 3 dB axial ratio bandwidth of dual band antenna is 4.57% and 4.27% for 3.5 GHz and 4.9 GHz respectively. The proposed antenna radiates in left hand circular polarization for lower frequency (3.5 GHz) and right hand circular polarization for higher frequency (4.9 GHz) with peak gain of 1.47 dBi and 1.33 dBi respectively. The antenna is fabricated using FR4 substrate having size of 30 mm × 30 mm. The parametric analysis of the design parameters has been carried out to optimize the performance of antenna. The fabricated prototype is tested and measured impedance bandwidth is around 60%. The measured and simulated results are found in close agreement with each other. The novelty of this research work is the transmission line equivalent circuit of proposed CPW fed antenna structure is presented and discussed.

Index Terms- Broadband, circularly polarized, dual sense, Y-shaped.

I. INTRODUCTION

In the last couple of years, circularly polarized (CP) planar microstrip antennas have grabbed vantage attention. In modern dynamic wireless communication technology, low cost, compact antennas with broad bandwidth is desired. Microstrip patch antennas (MPAs) with advantages of low profile, planar structure, ease of fabrication and comfortableness in polarization design are found suitable for wireless applications. CP MPAs are gaining popularity as they are resistant to multi-path fading effect and orientation of antennas [1]. Planar MPAs are found good candidate for modern wireless

communications as they can radiate in both directions. Recently, many investigations have been carried out to design dual band and dual band-dual sense CP MPAs with wide impedance and axial ratio bandwidth [2-13].

An array of hexagonal patch antennas along with annular feed network has been presented to realized dual sense CP [2]. In recent, authors have reported dual band CP printed monopole with L-shaped slot in ground and parasitically coupled diagonally square slot cut square shaped microstrip patch antenna for WLAN and vehicular communication applications [3]. An offset fed wideband inverted L -shaped strip loaded square slot antenna has been reported in [4]. To realize dual band dual sense CP, CPW fed square slot antenna with two parasitic patches [5], a semicircular patch with circular curved slot [6], swastika shaped aperture coupled dielectric resonator antenna [7], asymmetric square shaped ring along with dielectric resonator antenna [9], CPW fed monopole with two parasitically coupled rectangular radiators and I-shaped stub loaded antenna [10], asymmetrical square slot loaded L-shaped [11], U-shaped slot and stub loaded modified ground antenna are reported [13] in literature.

In the proposed research work, a new coplanar waveguide (CPW) fed dual asymmetric Y- shaped microstrip patch antenna for dual band dual sense CP operation with wide impedance bandwidth of 2.8 GHz (3- 5.8 GHz) covering WLAN and Wi-MAX wireless applications is proposed. The antenna consists of dual asymmetric Y- shaped patches to realized dual band dual sense CP. By proper tuning of length of ground plane, broad impedance bandwidth has been realized. The antenna has been fabricated using economical FR4 substrate having thickness $h = 1.6$ mm, $\epsilon_r = 4.3$, and $\tan \delta = 0.02$ with overall size of 30 × 30 mm². The



designed antenna has been simulated using method of moments based CAD FEKO simulator [14]. Standard SMA connector is used to feed this antenna. The fabricated antenna has been tested and measured results are found in close agreement with simulated results. First, single asymmetric Y-shaped antenna has been studied. This antenna offers broad impedance bandwidth of about 1.75 GHz with CP response at 3.54 GHz, having 220 MHz of axial ratio bandwidth. Further, additional asymmetric Y-shaped patch is added to yield dual band dual sense CP response with wide impedance bandwidth.

II. DESIGN OF ASYMMETRIC Y-SHAPED MICROSTRIP ANTENNA

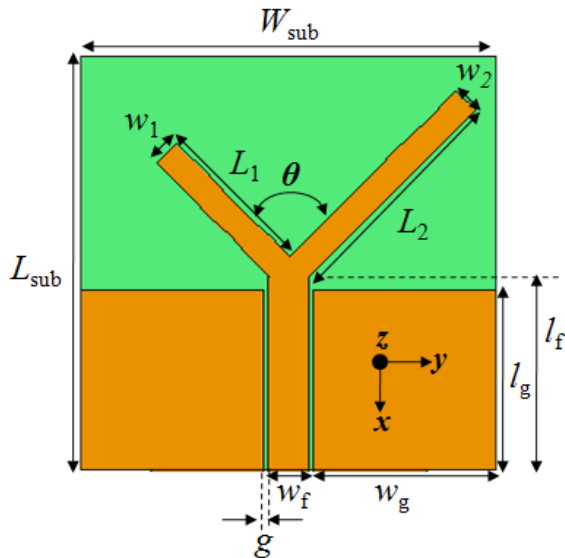


Fig. 1. Geometry of asymmetric Y-shaped microstrip patch antenna.

Fig. 1 presents geometry of asymmetric Y-shaped microstrip patch antenna for circular polarized response. The antenna is fed by coplanar wave guide (CPW) technique. The lengths of Y-shape patch designated as L_1 and L_2 is calculated using equation (1) and (2) respectively, to form symmetrical Y-shaped MPA.

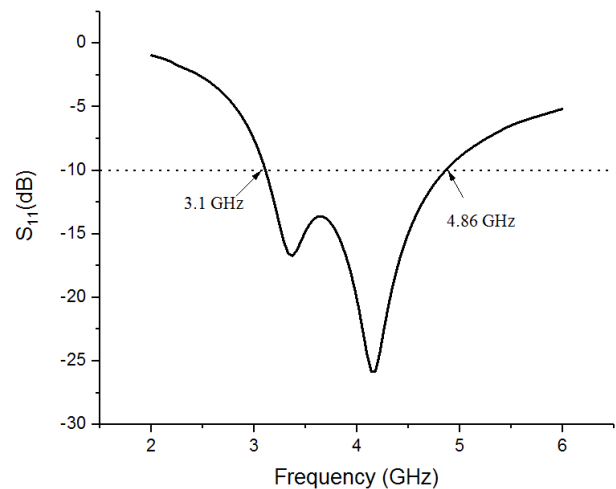
$$L = \frac{\lambda_0}{4\sqrt{\epsilon_{re}}} \quad (1)$$

$$\epsilon_{re} = \frac{\epsilon_r + 1}{2} \quad (2)$$

In equations (1) and (2), λ_0 is free space wavelength, ϵ_r is dielectric constant of substrate used and ϵ_{re} is the effective dielectric constant. The widths of Y-shaped patch and angle between the lengths L_1 and L_2 has been optimized using parametric analysis to improve CP performance of antenna. The length L_2 of Y-shaped antenna has been taken higher than L_1 to realize CP. However, the angle (θ) between lengths L_1 and L_2 has been varied to get optimum CP performance. The details of designed parameters of proposed antenna are given in Table 1.

Table 1: Design parameters of asymmetrical 'Y'-shaped MPA and measured (Fig. 1)

Parameter	Value (mm)
L_{sub}	30
W_{sub}	30
L_1	13
w_1	2
L_2	18
w_2	2
h	14
w_f	3
l_g	13
w_g	13.2
g	0.3
θ	90°



(a)

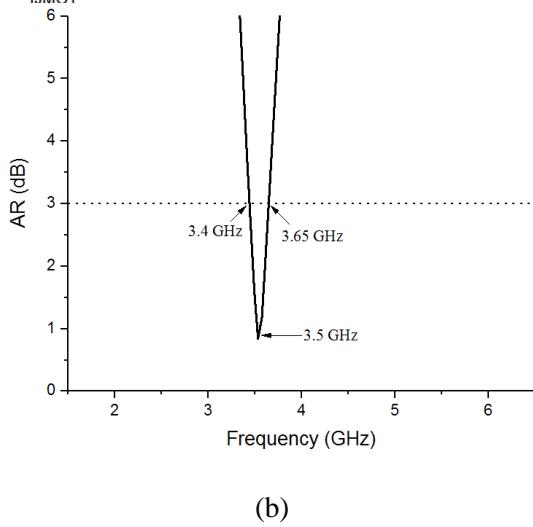


Fig.2. (a) Return loss (S_{11}) (b) axial ratio characteristics of asymmetric Y- shaped MPA

Fig. 2. depicts simulated return loss and axial ratio characteristics of asymmetrical Y- shaped MPA. The antenna offers 44.2% impedance bandwidth and 7.1% of axial ratio bandwidth. This asymmetric Y- shaped MPA covers Wi-MAX frequency band from 3.4–3.69 GHz. The detailed study of this antenna has been carried out using parametric analysis, by varying the lengths, widths and angle between the patches.

A. Parametric Analysis of Asymmetric Y-shaped MPA

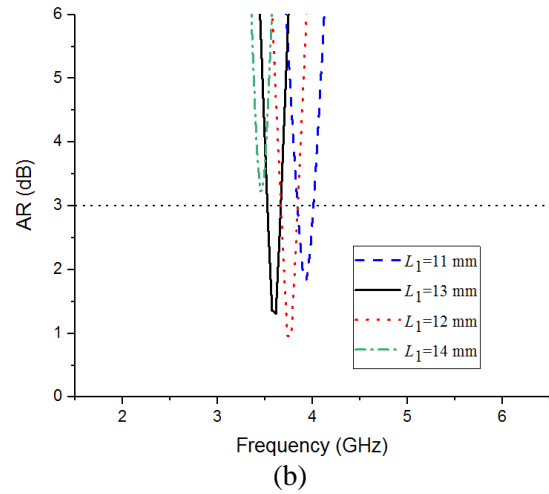
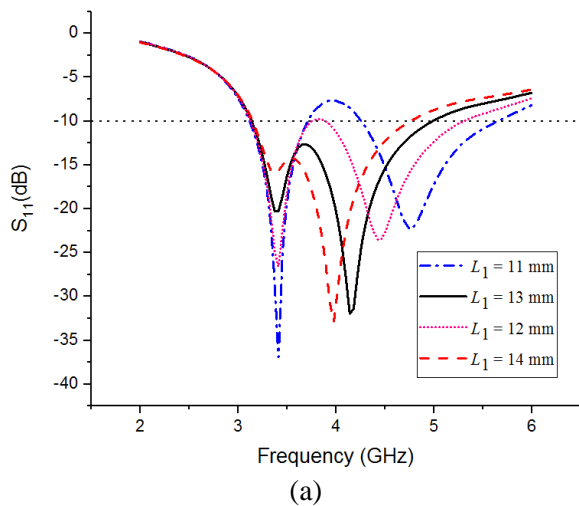
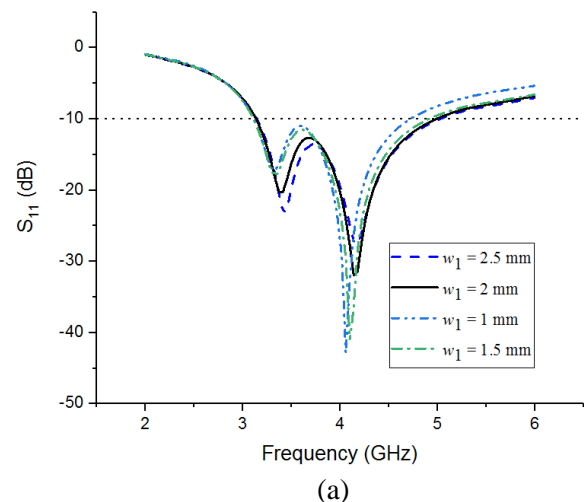


Fig.3. (a) Return loss (S_{11}) and (b) axial ratio characteristics of MPA with variation in L_1

Fig. 3 presents return loss and axial ratio characteristics of asymmetrical Y- shaped MPA for variation in length L_1 . The calculated value of length L_1 using equations (1) and (2) is 13 mm, which is equal to quarter wavelength at center frequency of 3.5 GHz. As depicted in fig. 3 (b), for $L_1 = 13$ mm, optimum axial ratio bandwidth has been realized. For lower value of length L_1 resonance frequency shifts towards higher side and realize dual band response as presented in Fig. 3(a). The parametric analysis has carried out for width w_1 . It has been observed that, for maximum value of $w_1 = 2.5$ mm, axial ratio shifts to higher side and impedance bandwidth decreases as depicted in Fig. 4. Therefore, an optimum value of $w_1 = 2$ mm has been selected.



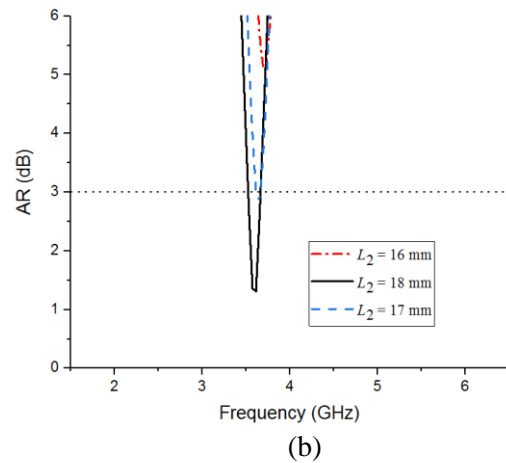
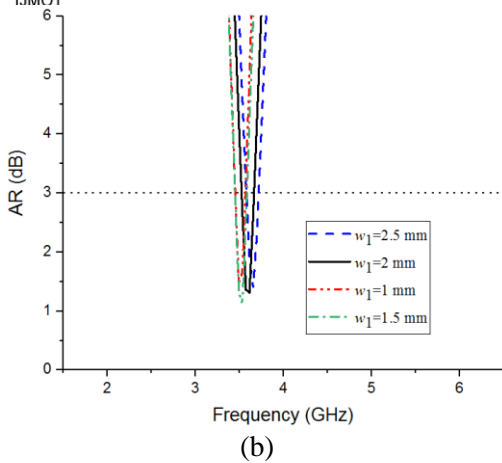


Fig. 4. (a) Return loss (b) axial ratio characteristics of variation of w_1

Fig. 5 and 6 depicts effect of variation of length L_2 and w_2 on return loss and axial ratio characteristics respectively. To realize CP, length of L_2 has been varied from 16 mm to 18 mm. It is studied that, for $L_2 = 18$ mm, maximum impedance bandwidth of 44.2% (1.76 GHz) and optimum CP performance has been realized. Similarly, for higher value of w_2 , optimum CP performance has been realized. However, lower impedance bandwidth has been realized with dual band response. It is also observed that, for lower value of w_2 , antenna does not exhibit CP performance. Therefore, optimum value of $w_2 = 2$ mm has been selected to realized maximum impedance bandwidth and better CP performance.

Fig.5. (a) Return loss and (b) axial ratio of variation of L_2

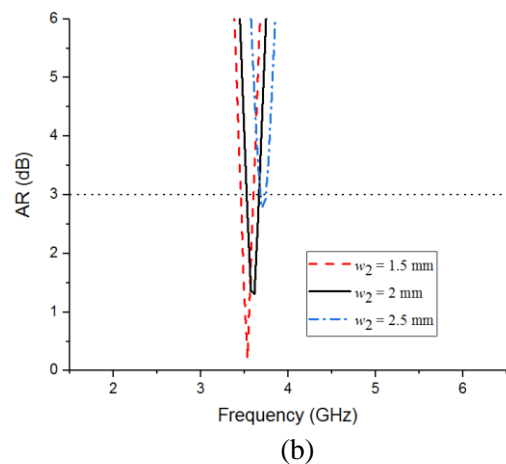
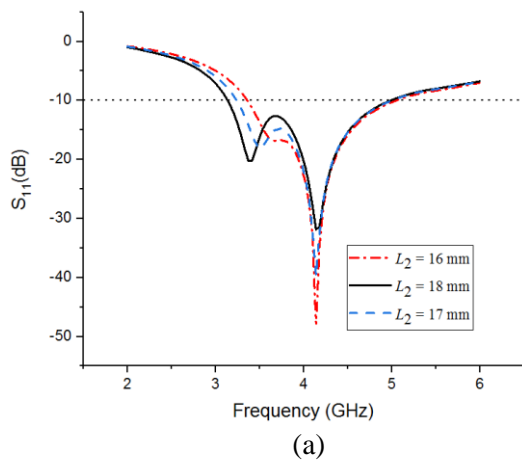
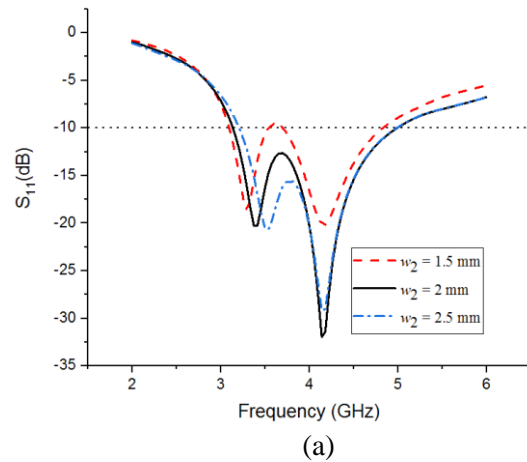


Fig.6. (a) return loss and (b) axial ratio of variation of w_2

The CP characteristics are realized by selecting asymmetry in lengths of Y- shaped patch. However, it is observed that, by varying the angle between the Y- shaped patch, CP performance can be improved. The angle between the Y- shaped patch denoted as ' θ ' has been varied from 60° to 90° . For the variation of specified range of angles, antenna exhibits CP performance. For $\theta = 80^{\circ}$, maximum impedance bandwidth of 56% has been realized. However, better CP performance has been obtained for $\theta = 90^{\circ}$ as depicted in Fig. 7 (a) and (b). The impedance characteristics has been also studied and it is observed that, a loop is formed inside VSWR circle indicating there is small parasitic coupling between lengths L_1 and L_2 due to gap created by angle ' θ ', when excited by CPW feed as presented in Fig. 8.

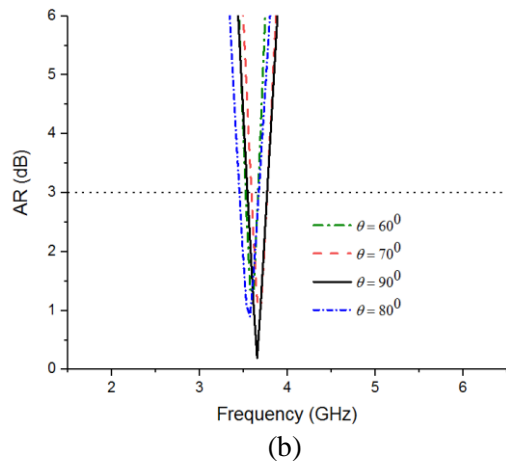
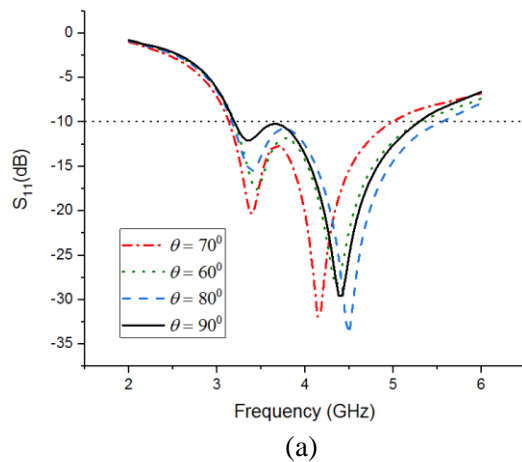


Fig. 7. (a) Return loss (b) axial ratio for variation of angle ' θ '

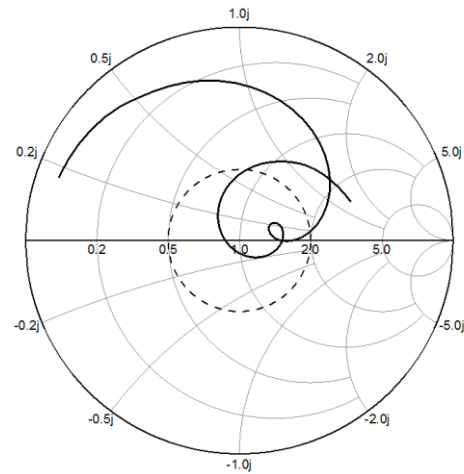


Fig. 8. Input impedance plot of asymmetric Y-shaped MPA

The radiation characteristics and current distribution of asymmetric Y- shaped MPA has been depicted in Fig. 9 (a)-(d).

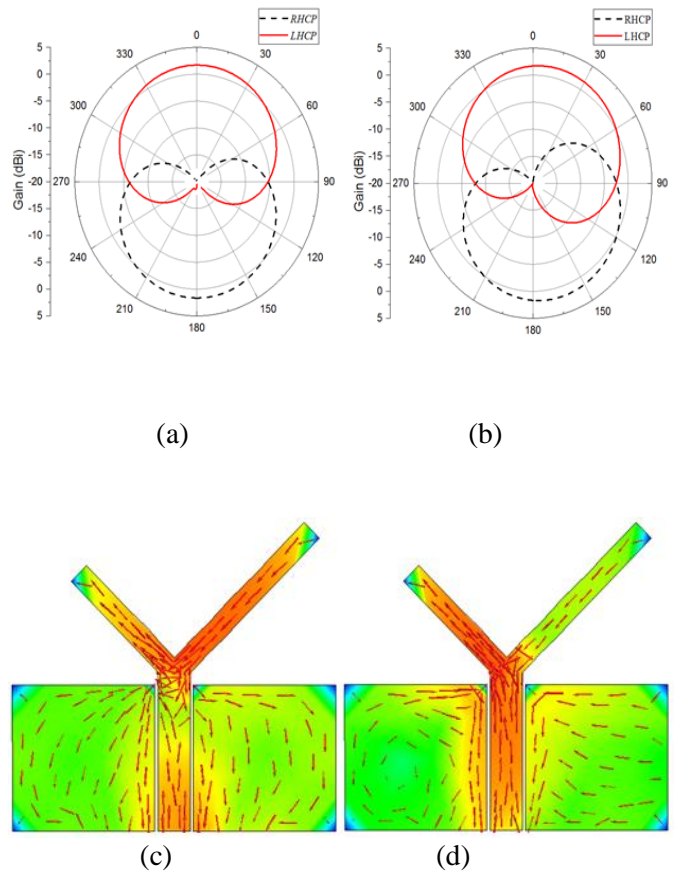


Fig. 9. (a) E-Plane (b) H-Plane Radiation pattern and (c) 0° (d) 90° surface current at 3.5 GHz

As presented in Fig. 9, this antenna offers left hand circular polarization (LHCP) at 3.5 GHz center frequency. The realized peak value of gain at 3.5 GHz is 1.47 dBi. The radiation property of this antenna can be verified by studying surface current presented in (c) and (d) for 0° and 90° respectively. The surface current is rotating in clockwise direction indicating antenna exhibits LHCP. From surface current distribution it is also observed that, for 0° , maximum current density lies inside length L_2 , whereas, for 90° , L_1 carries maximum current as CP field rotates through asymmetrical Y- shaped patch.

III. DESIGN OF DUAL ASYMMETRIC Y-SHAPED MICROSTRIP PATCH ANTENNA

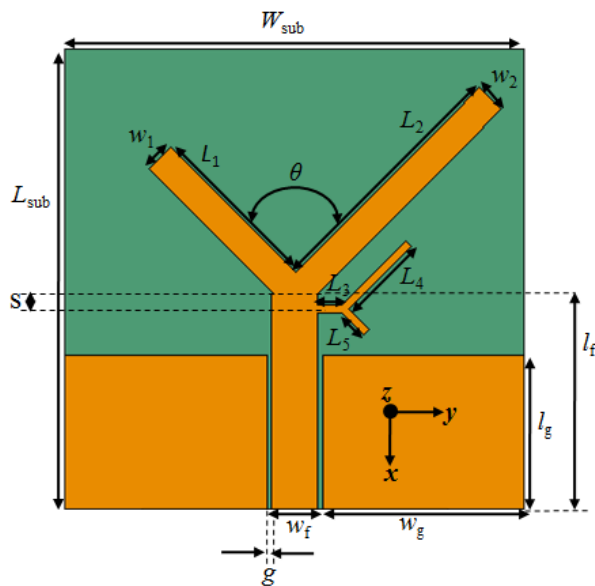


Fig. 10. Geometry of dual asymmetric Y- shaped MPA

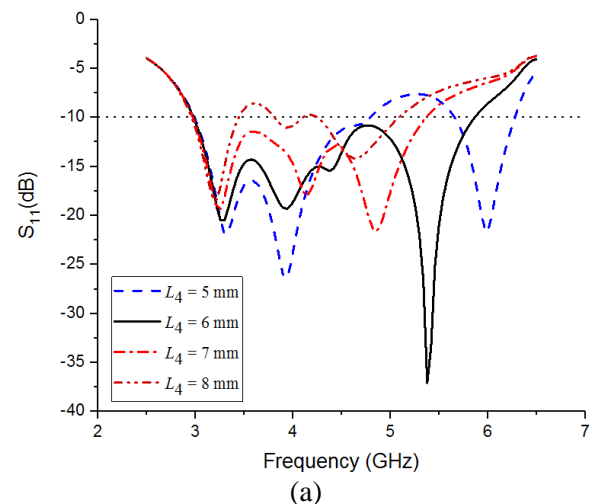
Fig. 10 depicts geometry of dual asymmetric Y-shaped MPA to realize dual band dual sense CP operation. To realize dual band dual sense CP, additional asymmetric Y- shaped patch has fed using microstrip line L_3 at an appropriate location. The length L_4 has been calculated using equations (1) and (2) for center frequency of 6 GHz. To realize RHCP at higher frequency, length of L_5 has been taken smaller than L_4 . The length of ground

plane l_g has been fine tuned to realize broad impedance bandwidth. The additional asymmetric Y- shaped patch has been fed using microstrip line near length L_2 , as fringing fields are more due to larger length of L_2 as compared to L_1 . The novelty of this research work is in independent tuning at both CP resonating frequencies. Further, to optimize performance of dual band dual sense CP, parametric analysis has been carried out for L_4 , L_5 , l_g and vertical distance 's' of microstrip feed line L_3 . The parameters of additional asymmetric Y- shaped MPA is summarized in Table 2. All previous design parameters are kept unchanged except length of ground plane l_g . To maintain the symmetry, the width of L_3 , L_4 and L_5 has been taken as 0.5 mm.

Table 2: Design parameters of additional dual asymmetric Y- shaped MPA (Fig.10)

Parameter	Value (mm)
L_3	2
L_4	6
L_5	2
s	0.75

Fig. 11 presents effect of change of L_4 on return loss and axial ratio characteristics. It was observed that, for higher values of L_4 , antenna exhibits dual band resonance response. Similarly, in case of axial ratio, CP frequency varies from higher side to lower side as L_4 varies from 5 mm to 8 mm, while the axial ratio at lower frequency remains unchanged. This describes the novelty of proposed research work of independent tuning of lower and higher CP frequencies.



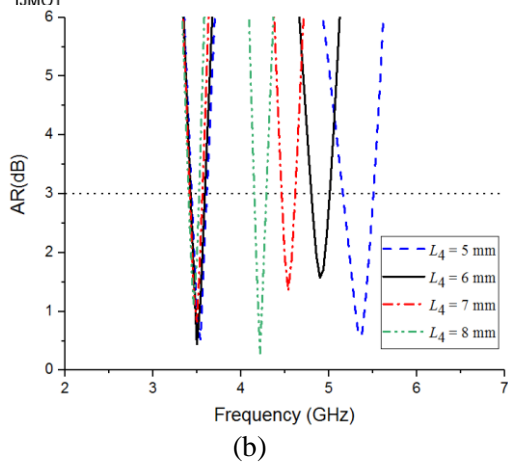


Fig. 11. (a) Return loss and (b) axial ratio characteristics of variation of L_4

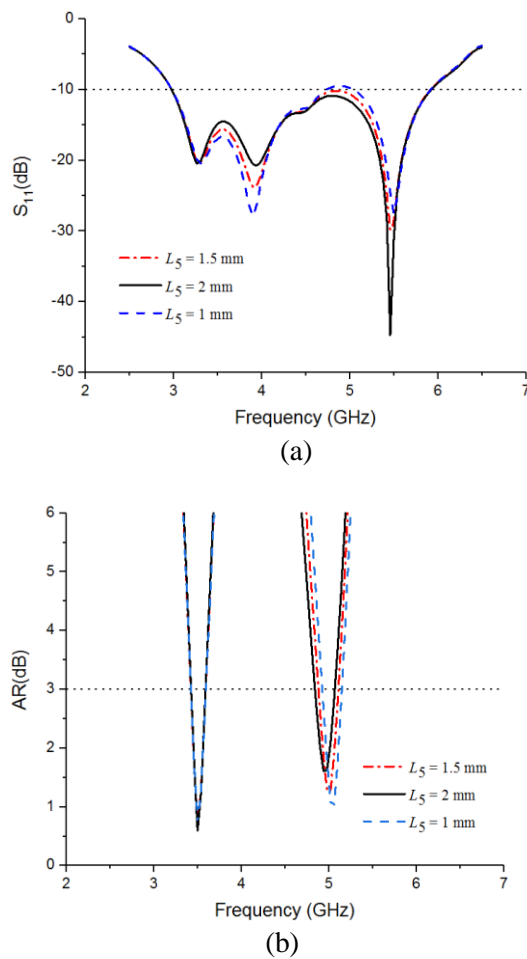


Fig. 12. (a) Return loss (b) Axial ratio characteristics of effect of L_5

The iterations of length at different values have been simulated and it has been observed that, variation of length L_5 , does not have significant impact on antenna performance. However, slight change in return loss and axial ratio frequency has been observed as presented in Fig. 12. It has been studied and observed that, the vertical location 's' of microstrip line L_3 has significant impact on return loss characteristics as depicted in Fig. 13. The value of vertical location 's' has been varied from $s = 0$, 0.25 and 0.75 mm and for $s = 0.75$ mm, antenna exhibits broadband resonance response. For the similar variations of 's', axial ratio slightly reduces towards lower frequency.

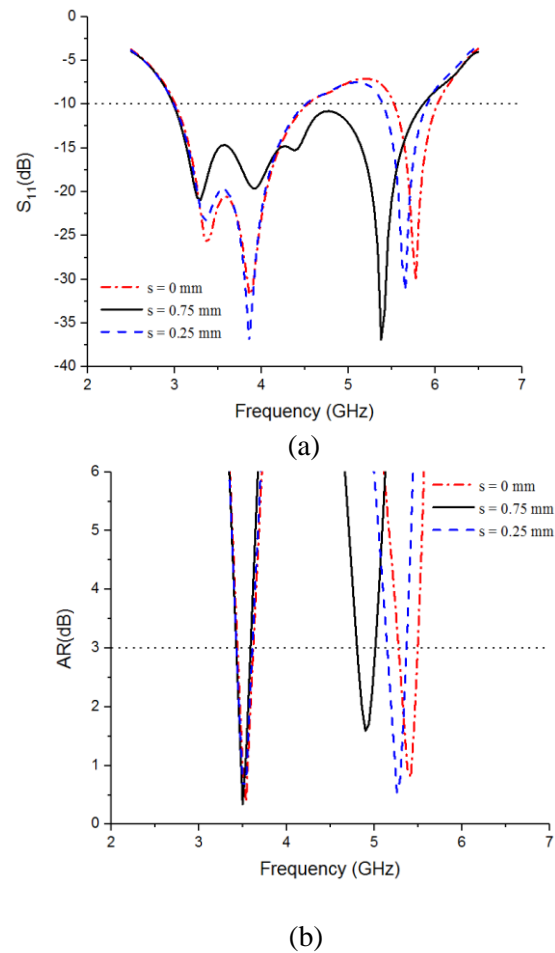


Fig. 13. (a) Return loss and (b) axial ratio characteristics of change in 's'

Fig. 14 depicts effect of length of ground plane on return loss and axial ratio characteristics. To study the effect of ground length variations, the value of ground length l_g has been varied from 8 mm to 11 mm. For lower values of ground length antenna exhibits dual band response. As the length of ground plane increase to 11 mm, antenna realizes broadband response with nearly 65% impedance bandwidth. For $l_g = 10$ and 11 mm, antenna exhibits CP response. However, optimum CP response has been realized for $l_g=11$ mm.

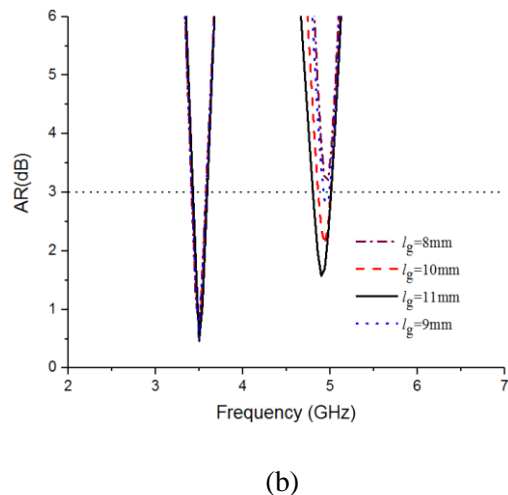
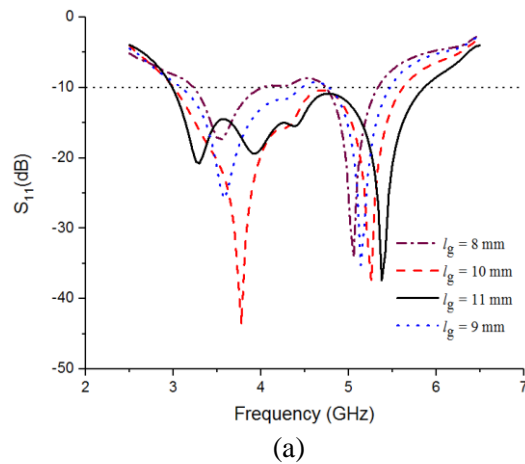


Fig. 14. (a) Return loss (b) axial ratio characteristics of variation in l_g .

As additional asymmetric Y-shaped patch has been used near length L_2 , there exist a small parasitic coupling between L_2 and L_4 .

This can be verified by studying the impedance loop as shown in Fig. 15. Two small closed loops inside VSWR circle has been formed indicating parasitic coupling between $L_1 - L_2$ and $L_2 - L_4$ respectively.

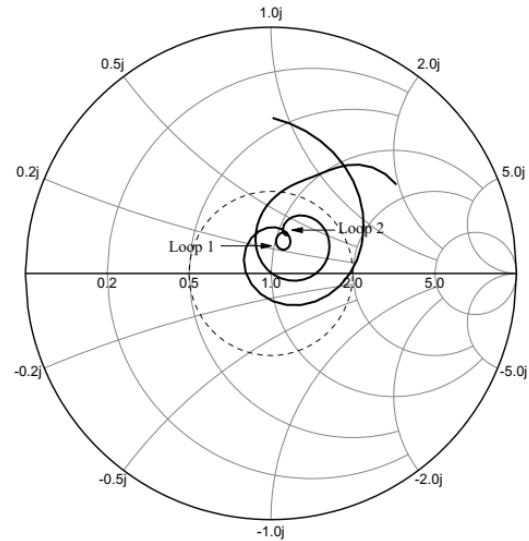


Fig. 15. Impedance plot of dual asymmetric Y-shaped MPA

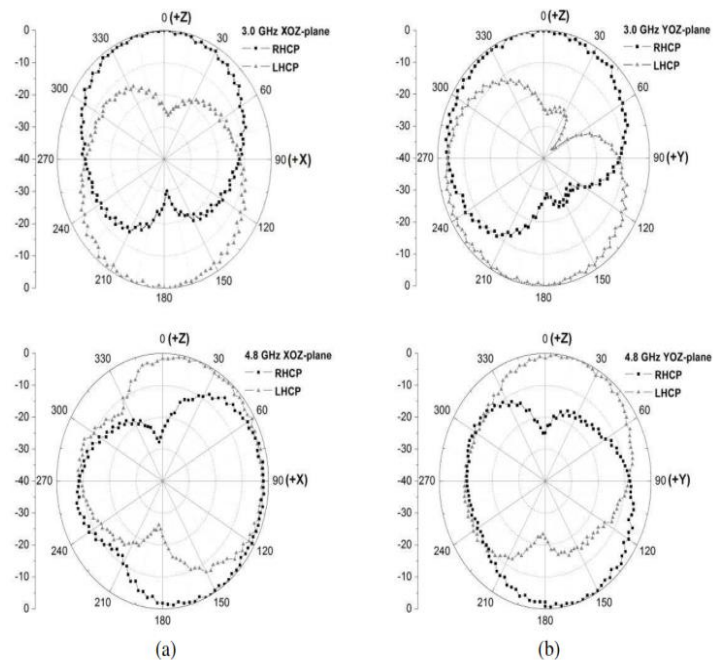


Fig. 16. Measured radiation pattern reported in [13]

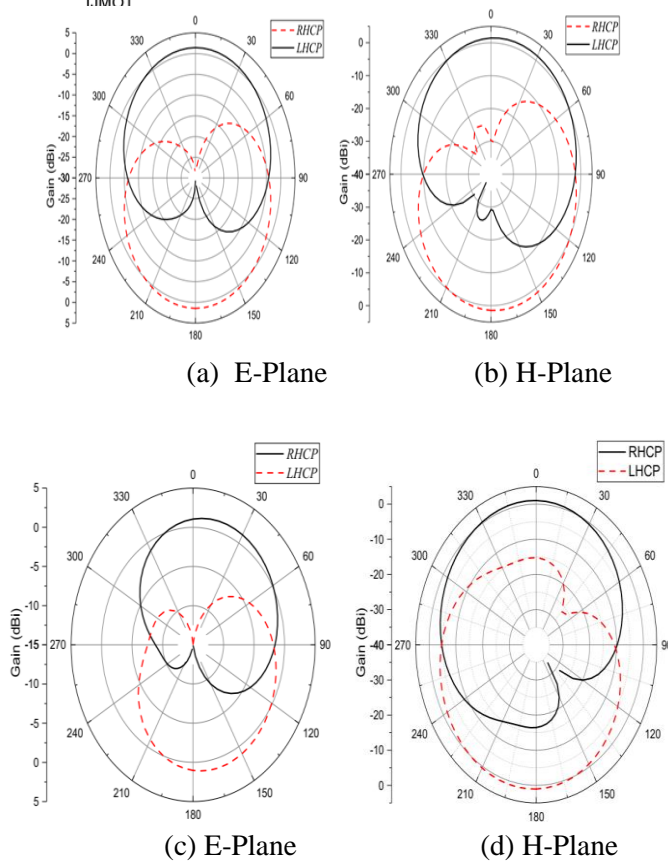


Fig. 17. Radiation pattern of proposed dual 'Y' shaped MPA (a-b) 3.5 GHz and (c-d) 4.9 GHz

Fig. 16 presents measured radiation pattern reported by chen and Zhang [13]. Fig. 17 represents simulated radiation pattern of proposed dual Y- shaped MPA. The pattern describes the radiations are in LHCP in + z direction for lower frequency band and RHCP at higher frequency band in + z direction. Thus, realizing dual band dual sense CP operation. The radiations at both the frequencies are in broadside directions with maximum gain of 1.47 dBi at lower frequency and 1.33 dBi at higher frequency. It has been observed that, the radiation at higher frequencies is slightly tilted. This may be because of asymmetry in Y-shaped structure designed to realize higher frequency. The simulated radiation pattern of proposed antenna has been compared with measured radiation pattern reported in [13] for experimental validation and comparison between proposed antenna and previously reported antenna structure exhibiting similar dual band dual sense characteristics. It is observed that, measured radiation pattern reported in [13] exhibits RHCP at 3.0 GHz and LHCP at 4.8 GHz with gain of 3.0 and 1.4 dBic respectively. Whereas, proposed antenna structure exhibits LHCP at 3.5 GHz and

RHCP at 4.9 GHz with gain of 1.47 and 1.33 dBi respectively. As mentioned in [13], the cross polarization level is below 24 and 25 dB for lower and higher frequencies respectively. Whereas in proposed antenna structure, cross polarization is below 20 dB for lower and higher frequency. This difference in cross polarization may be due to larger ground plane in proposed antenna design. The surface current distribution of proposed antenna is presented in Fig. 18. At lower frequency rotation of current is in clockwise direction and at higher frequency rotation is in anti-clockwise realizing LHCP and RHCP respectively.

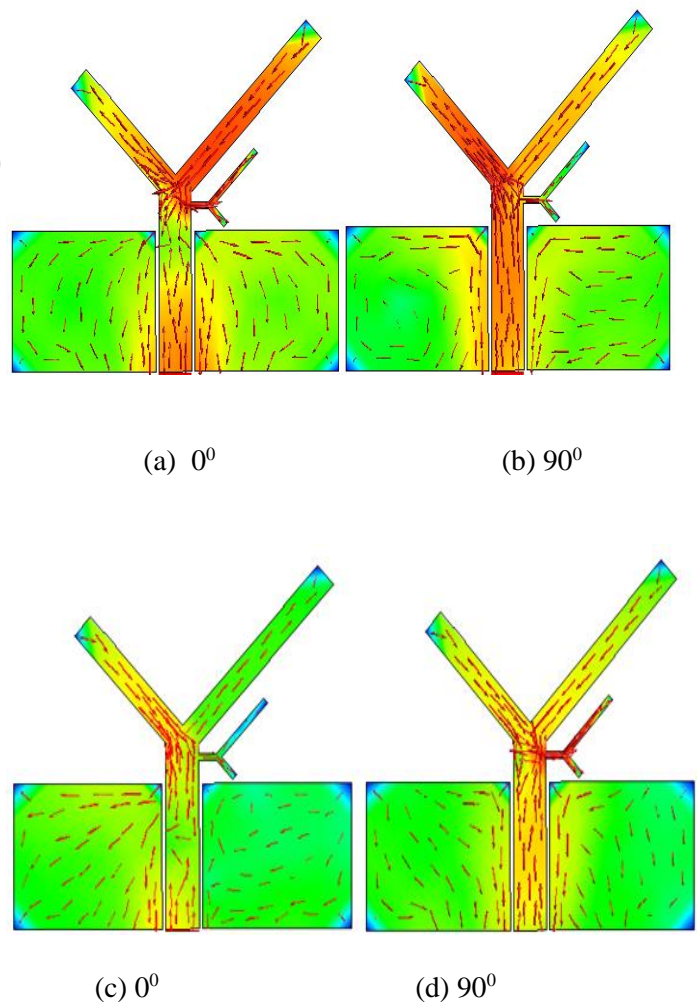


Fig. 18. Surface current (a-b) 3.5 GHz, (c-d) 4.9 GHz

IV. EQUIVALENT CIRCUIT ANALYSIS OF PROPOSED ANTENNA

The theoretical analysis of proposed CPW fed dual asymmetric Y-shaped antenna has been prepared and its transmission line equivalent circuit is



presented in Fig. 19. In this analysis, the asymmetric single Y-shaped and dual Y-shaped antenna and its equivalent circuit parameters are analyzed and calculated. The CPW transmission line model is prepared which acts as impedance matching line. The proposed CPW line is modelled and represented by two series inductors L_{ML1} and a shunt capacitor C_{ML1} respectively [15]. The single asymmetric Y-shaped patch is modelled as parallel R, L, C circuit. The patch, L_1 , w_1 and L_2 , w_2 are represented as L_1 , C_1 , R_1 and L_2 , C_2 and R_2 and their values are calculated using equations (3) and (4) respectively [3]. The calculated values for L_1 and C_1 is $1.21 \mu\text{H}$ and $1.72 \times 10^{-15} \text{ F}$ respectively. Similarly, $1.68 \mu\text{H}$ and $1.24 \times 10^{-15} \text{ F}$ are the values calculated for L_2 and C_2 respectively.

There exists a parasitic capacitance between two asymmetrical lengths of single Y-shaped patch which is calculated using equation (5) [15-16]. The obtained value of parasitic capacitance between single asymmetric Y-shaped patches is $C_{p1} = 47.59 \text{ pF}$.

$$L_1 = \frac{1}{C_1 \omega_0^2} \quad (3)$$

$$C_1 = \frac{2w\epsilon_r}{Lh\omega_0^2} \quad (4)$$

$$C_p = \epsilon_0 \epsilon_r \frac{w}{h} \quad (5)$$

In equations (3) - (5), ω_0 is angular frequency, w is width of asymmetric Y-shaped patches, L is length of respective patch, h the substrate thickness, ϵ_r relative permittivity of substrate and $\epsilon_0 = 8.854 \times 10^{-12} \text{ F}$. Similar analysis has been carried out for another asymmetrical Y-shaped patch, in which length L_3 is modeled as transmission line equivalent circuit and represented by L_{ML2} and C_{ML2} , patches L_4 and L_5 are modelled as L_3 , C_3 , R_3 , and L_4 , C_4 , R_4 respectively. The calculated values are $C_3 = 3.76 \times 10^{-16} \text{ F}$, $L_3 = 2.23 \mu\text{H}$, $C_4 = 1.12 \times 10^{-15} \text{ F}$ and $L_4 = 0.75 \mu\text{H}$. The parasitic capacitances between length $L_4 - L_5$ and between $L_2 - L_4$ is estimated

using equation (5) and calculated as $C_{p3} = 11.89 \text{ pF}$ and $C_{p2} = 29.74 \text{ pF}$ respectively.

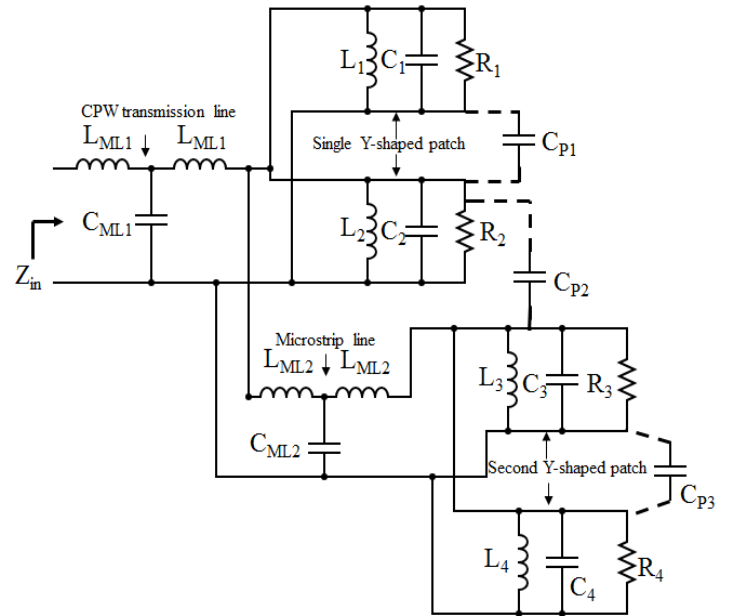


Fig. 19. Equivalent circuit of asymmetric dual Y-shaped MPA

V. EXPERIMENTAL VERIFICATION AND DISCUSSION

The proposed antenna samples with optimized dimensions is fabricated and tested using FieldFox N9916A vector network analyzer (VNA). The fabricated prototypes are depicted in Fig. 20. The simulated and measured return loss characteristics of asymmetric Y-shaped and dual Y-shaped antennas are compared and presented in Fig. 21 with experimental setup in inset.

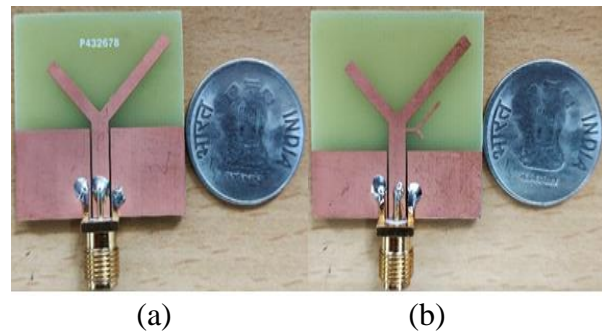
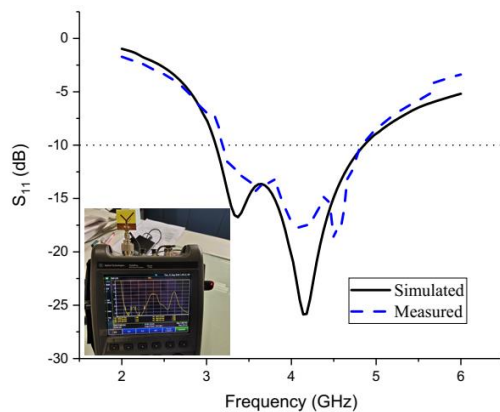
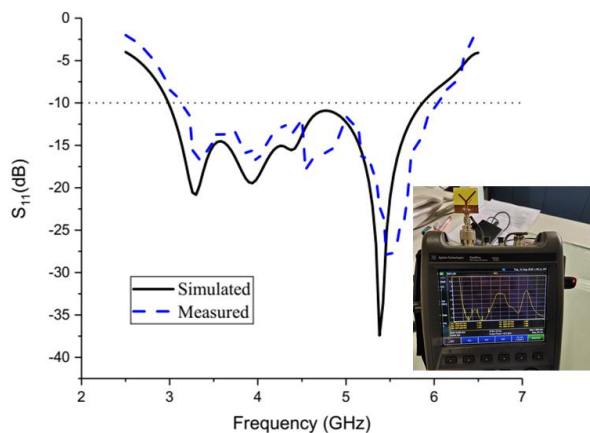


Fig. 20. Fabricated prototypes (a) Asymmetric Y-Shaped MPA (b) Asymmetric dual Y-shaped MPA

The measured impedance bandwidth is 40% (1.6 GHz) and 60% (2.75 GHz) for asymmetric single Y- and dual Y- shaped microstrip patch antennas respectively. The simulated and measured results of return loss characteristics are in close agreement. The S_{11} magnitude of measured result is slightly less than simulated. This may be because of fabrication tolerances. The antenna realizes broadband response covering Wi-MAX (3.4-3.69 GHz), WLAN (5.15-5.35 GHz and 5.725 – 5.825 GHz) wireless application services.



(a) Single Y-shaped microstrip patch antenna



(b) Dual Y-shaped microstrip patch antenna

Fig. 21. Comparison of simulated and measured return loss characteristics with experimental setup in inset (a) Single Y- shaped MPA (b) Dual Y- shaped MPA

The proposed research work has been compared with previously reported work of dual band dual sense circularly polarized microstrip antennas. This comparative analysis has been presented in Table 3.

Table 3: Comparison of present work with previously reported research work

Parameter	Size (m ²)	ARBW (%)		Imp.BW (%)		CP freq. ratio	Pol.		Gain (dBic/dBi)	
		Lower	Higher	Lower	Higher		Lower	Higher	Lower	Higher
[4]	50x50	55	29.3	111		2.2	RH CP	LH CP	4.2	3.4
[9]	60x50	11.6	5.86	55.18		1.25	RH CP	LH CP	3.05	1
[11]	60x50	37.4	16.3	38.8	27.5	1.83	RH CP	LH CP	4.3	3.3
[13]	60x50	28.4	26.3	18.3	23.7	1.8	RH CP	LH CP	3	1.4
Proposed Work	30x30	4.57	4.27	60		1.4	LH CP	RH CP	1.47	1.33

*BW = bandwidth, Imp = Impedance

VI. CONCLUSION

In this research work, dual band dual sense circularly polarized microstrip patch antennas are designed, simulated and tested. New designs of asymmetric single and dual Y- shaped structure are proposed to realize dual band dual sense circular polarization. The antenna exhibits broadband response having 40 % and 60% of measured impedance bandwidth for single and dual asymmetric Y- shaped patches respectively. The antenna also offers independent frequency tuning of circular polarization at 3.5 GHz and 4.9 GHz frequencies. The radiation patterns of antennas are in broadside direction with peak gain of 1.47 dBi and 1.33 dBi. The measured and simulated results are compared and found in close agreement with each other.



The transmission line equivalent circuit for proposed antenna structure is presented and analyzed. The proposed antenna structure can be useful for various wireless service such as WLAN, Wi-MAX and vehicular communications.

ACKNOWLEDGMENT

Mandar P. Joshi is highly indebted to Management and Principal, G.E.S's R. H. Sapat College of Engineering, Management Studies and Research, Nashik, India for granting him to pursue Ph.D under Savitribai Phule Pune University, Pune, India. Technical support from Sonic Multitech Pvt. Ltd, Nashik, India is thankfully acknowledged.

REFERENCES

- [1] S. Gao, Q. Luo and F. Zhu, *Circularly Polarized Antennas*, John Wiley & Sons, 2014.
- [2] Y. Zheng, M. Gao and X. Zhao, "A Novel Patch Array Antenna with Wideband and Dual Sense Circular Polarization Characteristics for WiMAX and WLAN Applications," *Progress in Electromagnetic Research C*, Vol. 99, pp. 123-132, January, 2020.
- [3] Mandar P. Joshi, Vitthal J. Gond, "Design and Analysis of Microstrip Patch Antenna for WLAN and Vehicular Communication," *Progress in Electromagnetic Research C*, Vol. 97, pp. 163-176, December, 2019.
- [4] R. Xu, J.-Y. Li, J. Liu, S. -G. Zhou, K. Wei and Z. -J. Xing, "A Simple Design of Compact Dual-Wideband Square Slot Antenna with Dual Sense Circularly Polarized Radiation for WLAN. Wi-Fi Communications," *IEEE Transactions on Antennas and Propagation*, Vol. 66, No. 9, pp. 4884 – 4889, September, 2018.
- [5] Rohit kumar Saini, Pritam Singh Bakaria, Pawan Kumar, "Coplanar Waveguide Fed Dual Band Dual Sense Circular Polarized Square Slot Antenna," *International Journal of RF and Microwave Computer-Aided Engineering*, Wiley, pp. 1-8, September, 2018 DOI:10.1002/mmce.21503.
- [6] Huy Hung Tran, Tuan Tu Le, Truong Khang Nguyen, "Dual Band Dual Sense Circularly Polarized Antenna for S and C Band Applications," *Microwave and Optical Technology Letters*, pp. 1-6, November, 2018, DOI: 10.1002/mop.31546.
- [7] Anand Sharma, D. K. Tripathi, Gourab Das, R. K. Gangwar, "Novel Asymmetrical Swastik- Shaped Aperture Coupled Cylindrical Dielectric Resonator Antenna with Dual Band Dual Sense Circular Polarization Characteristics," *Microwave and Optical Technology Letters*, pp. 1-7, November, 2018, DOI: 10.1002/mop.31554.
- [8] Hasan Saygm, Vahid Rafiei, Saeid Karamzadeh, "A New Compact CP Antenna Design," *Microwave and Optical Technology Letters*, pp. 594-600, February, 2018, DOI: 10.1002/mop.31019.
- [9] Nilesh Kumar Sahu, Anand Sharma, R. K. Gangwar, "Design and Analysis of Wideband Composite Antenna with Dual Sense Circular Polarization Characteristics," *Microwave and Optical Technology Letters*, pp. 2048 – 2054, June, 2018 DOI:10.1002/mop.31293.
- [10] Rohit Kumar Saini, Santanu Dwari and Mrinal Kanti Mandal, "CPW Fed Dual Band Dual Sense Circularly Polarized Monopole Antenna," *IEEE Antennas and Wireless Propagation Letters*, Vol. 16, pp. 2497 – 2500, July, 2017. DOI: 10.1109/LAWP.2017.2726545.
- [11] Xu Rui, Jianying Li and Kun Wei, "Dual Band Dual Sense Circularly Polarized Slot Antenna with Simple Structure," *Electronic Letters*, Vol. 52, No. pp. 578-580, April, 2016.
- [12] Yonghao Xin, Quanyuan Feng and Jun Tao, "A CPW Fed Dual Band Slot Antenna with Circular Polarization," *Progress in Electromagnetic Letters*, Vol. 61, pp. 77-83, July, 2016.
- [13] Bo Chen and Fu-Shun Zhang, "Dual Band Dual Sense Circularly Polarized Slot Antenna with an Open Slot and a Vertical Stub," *Progress in Electromagnetic Research Letters*, Vol. 48, pp. 51-57, August, 2014.
- [14] Altair's Hyperworks CAD FEKO, Altair Engineering Inc. USA.
- [15] R. Garg, P. Bhartia, I. Bahl and A. Ittipiboon, *Microstrip Antenna Design Handbook*, Artech House, Norwood, M.A., 2000.
- [16] Mandar P. Joshi, Jayant G. Joshi and Shyam S. Pattnaik, "Stub Loaded Rectangular Ring Shaped Tri-Band Monopole Antenna for Wireless Applications," *International Journal of Advances of Microwave Technology*, Vol. 5, No.2, pp. 227 – 233, May, 2020.